Comprehensive Assessment of Nitrogen Dioxide Concentration Dynamics in Konkan Region, India

Aman Srivastava[1], Aditya Kumar Thakur[1], Pritipadmaja[1], Rahul Dev Garg[1], Pradeep Kumar Garg[1]

[1]Department of Civil Engineering, Indian Institute of Technology Roorkee, Haridwar, India - aman_s1@ce.iitr.ac.in; aditya_kt@ce.iitr.ac.in; pritipadmaja@ce.iitr.ac.in; rdgarg@ce.iitr.ac.in; p.garg@ce.iitr.ac.in

Keywords: Konkan Region Pollution, Sentinel-5P, Global Moran's I, Hotspot Analysis, Hazard Zonation.

Abstract

Air pollution is a primary environmental concern mainly in urban areas. Previous research on air pollution in the Konkan region has primarily focused on ground-based measurements, often lacking comprehensive spatial coverage and long-term trend analysis. This study uses satellite data of Sentinel-5P to examine the spatiotemporal trends and hazard zonation of NO_2 concentrations in the Konkan region of Maharastra from 2019 to 2023. Various statistical tools such as central tendency and other parameter estimation, along with correspondence analysis were used to assess the variability. The classification was done using the binary mask having a threshold of $0.9*10^{-4}$, and logical operation was employed for hazard zonation. The classification reveals 2,065 sq. km. of the area under the highest hazard level. The analysis also highlighted that the mean NO_2 concentration rose from 0.7027×10^{-4} mole/m² in 2019 to 0.7680×10^{-4} mole/m² in 2023, with consistent spatial variability. It may be attributed to persistent emission sources like industrial zones and highways. Spatial correspondence analysis revealed strong associations between consecutive years but a decline over longer periods. However, the overall association value was quite high over the study period. Persistent pollution is observed in areas like Thane, Mumbai, Navi Mumbai, Washi, Dadar and Colaba, along with the highest level of hazard. It reflects the consistency of pollution over a certain area and the need for targeted intervention for pollution control and sustainable environmental development. Overall, this study underscores the significance of satellite-based monitoring for identifying pollution trends and hotspots. It also offers insights into evidence-based mitigation strategies to improve air quality and protect public health.

1. Introduction

Air pollution is a critical environmental issue, particularly severe in urban centers with high population densities as well as in mining and industrial regions. This severity is primarily attributed to intense industrial activities, vehicular emissions, energy production, and unregulated urban expansion, all of which contribute significantly to the deterioration of air quality (Chan and Yao, 2008; Gond et al., 2024; Gupta et al., 2024; Mishra et al., 2024; Sahu et al., 2020). Nitrogen dioxide (NO_2), a major pollutant, poses significant risks to air quality and public health. Prolonged exposure to elevated NO_2 levels can contribute to asthma development and increase susceptibility to respiratory infections, highlighting its serious environmental and health implications (Bose and Leitmann, 1996; Haque and Singh, 2017; Maltare and Vahora, 2023; Organization, 2021; Pandey et al., 2021). Studies in India reveal rising levels of pollutants like sulfur dioxide (SO_2), nitrogen oxides (NO_x), and particulate matter (PM2.5), with severe health consequences, mainly in urban and industrial areas. Researchers emphasize the requirement for enhanced monitoring and regulatory measures to safeguard public health (Meo et al., 2022; Sharma et al., 2019; Suthar et al., 2022).

Developing countries face economic challenges in addressing air pollution. A study analyzed tropospheric NO_2 over Tehran using Sentinel-5P data, revealing a 6% reduction in NO_2 levels in 2020 compared to 2019, attributed to COVID-19 restrictions. The most polluted areas were northern, northeastern, and central Tehran, with Pearson's correlation coefficients of 0.58 (2019) and 0.61 (2020) (Sharifi and Felegari, 2022). Another study shows NO_2, a key precursor to photochemical smog, has significantly increased in China due to rapid economic growth. Sentinel-5P TROPOMI data (2018–2019) reveal seasonal (higher in winter) and spatial (higher in the East) NO_2 patterns, with economic activities like industrial output and vehicle ownership strongly influencing concentrations. The findings guide region-specific NO_2 reduction strategies (Zheng et al., 2019).

In India, limited monitoring stations result in uneven air pollution data, highlighting the importance of satellite data like Sentinel-5P TROPOMI. This study analyzes spatial-temporal trends of key pollutants (2019–2022), showing NO_2 and SO_2 hotspots in megacities and industrial zones, with seasonal variations and notable lockdown-related reductions. Findings offer insights for hotspot identification and strategies to mitigate pollution, improve health, and enhance environmental quality (Mathew et al., 2024). A study analyzes spatio-temporal variations of tropospheric NO_2 and total CO in Punjab and Haryana, highlighting pollution hotspots like Delhi and Lahore using Sentinel-5P data. Winter pollution peaks due to crop residue burning and boundary layer effects, while the COVID-19 lockdown led to significant NO_2 reductions (up to 59%). Lockdown stringency moderately correlates with NO_2 levels, factoring in meteorological influences (Shabbir et al., 2024).

The COVID-19 lockdown in 2020 improved air quality across India, with significant reductions in NO_2, SO_2, HCHO, and aerosols compared to 2019. However, pollutant levels, including NO_2, SO_2, HCHO, and CO, rose in 2021 due to relaxed restrictions. Pyrogenic and agricultural sources influenced the air quality, particularly for HCHO, CO, and CH_4 (Behera et al., 2022). During the COVID-19 lockdown, while stratospheric ozone showed repair, lower atmospheric ozone (O_3) levels significantly increased over India, driven by emissions from sources like stubble burning. This study estimated O_3 concentrations over Pune using Sentinel-5P data and

compared Ordinary Least Squares (OLS) and Random Forest (RF) regressions, achieving high accuracy (R²: 0.90-0.968). The findings highlight the role of multiple factors influencing O_3 levels and the utility of satellite data for efficient estimation (Reshi et al., 2022).

Previous studies lack detailed spatiotemporal analysis and the study of the persistency of pollutants over a specific area. This study employed various statistical tools to investigate the distribution pattern and its temporal dynamics for the Konkan region. Parameters such as mean, extremes, and standard deviation for different years were used to assess the spatiotemporal variability of NO_2 over the study area. Further, the Global Morans Index was used to assess the association between the distribution zones over the years. Hazard zonation was done using the logical operation between the two class raster maps of different years. Two class maps were made using the binary mask, which divides the area into hazardous and non-hazardous. Overall, the study provides detailed information that can be used as effective pollution control measures in the Konkan region.
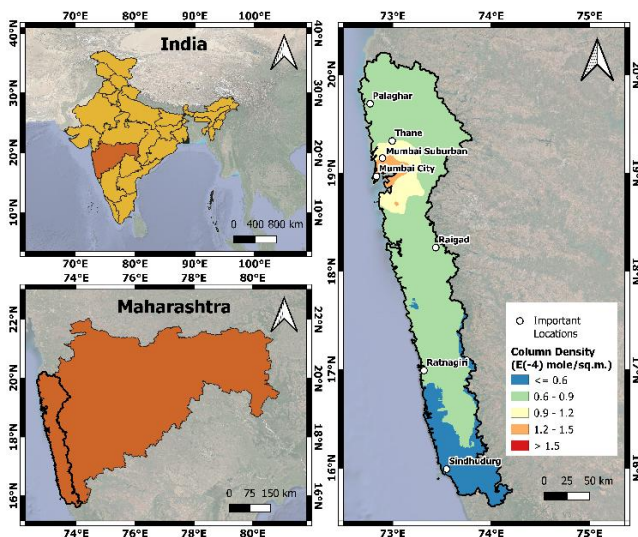
2. Study Area

Figure 1. Study area map of the Konkan region illustrating different NO_2 distribution classes based on mean value over five years. Important locations within the region are also shown.

The Konkan division, located along the western coast of India, stretches across Maharashtra, Goa, and Karnataka (Chore et al., 2021; Nayak and Hanamgond, 2010). The study area bound from 20.5° N (near Daman in Gujarat) to 15.5° N (near Karwar in Karnataka), and from 72.5° E (along the Arabian Sea coast) to 74.5° E (towards the Western Ghats). The region is known for its scenic landscapes, it includes lush forests, fertile plains, and pristine beaches (Borkar et al., 2018). The region experiences a tropical monsoon climate, which influences its rich biodiversity and agricultural activities, including rice, coconut, and cashew cultivation. Major urban centres like Mumbai and Goa contribute to the region's economic significance. Additionally, the Konkan is vulnerable to environmental challenges, including air pollution,

particularly in industrial and urban areas, making it a critical area for environmental monitoring and study (Doke, 2017).

The Konkan division of the Maharastra state, comprising Palghar, Thane, Mumbai Suburban, Mumbai City, Raigad, Ratnagiri, and Sindhudurg, experiences varying levels of environmental conditions influenced by urbanization, industrial activities, and its coastal geography (Figure 1). Palghar faces moderate pollution due to emissions from industries and vehicles, while Thane is affected by rapid urbanization and construction dust, leading to increased pollution. Mumbai Suburban and Mumbai City are heavily impacted by traffic congestion, industrial outputs, and dense urban settlements, contributing to significant environmental concerns. Raigad, with its mix of industrial hubs and semi-rural areas, experiences moderate pollution levels, while Ratnagiri and Sindhudurg benefit from their coastal winds, greenery, and limited industrialization, making them the least polluted parts of the region. Despite its natural advantages, the northern and central parts of the Konkan region are increasingly impacted by human activities, leading to noticeable environmental challenges.

3. Methodology

3.1 Dataset

Remote sensing satellite data, specifically Sentinel data, is crucial for hazard monitoring, providing high-resolution, real-time information on environmental changes. It aids in tracking disasters like floods, wildfires, land surface deformation, pollutants accumulation, and landslides, enabling timely responses and effective mitigation strategies (Bhattacharjee and Garg, 2024; Chowdhury and Dwarakish, 2022; Guptha et al., 2022; Hasan and Ahmed, 2023; Karanam et al., 2021; Kumar et al., 2022; Maurya et al., 2022; Mondal and Paul, 2023; Pritipadmaja et al., 2023; Sharifi and Felegari, 2022; Soudagar et al., 2025; Srivastava et al., 2025; Tang et al., 2024; Thakur et al., 2025a, 2025b, 2024; Verma and Vijay, 2024; Yaseen, 2024). Sentinel-5P satellite from the Copernicus program is efficient in monitoring atmospheric pollutants. It helps in providing high-resolution (resampled to 1 km*1 km) global measurements of various atmospheric gases (Bodah et al., 2022; Савенець et al., 2019). Sentinel5P satellite is part of the European Space Agency's (ESA) Copernicus Earth observation program and monitors air quality and atmospheric composition. It uses the Tropospheric Monitoring Instrument (TROPOMI) to capture detailed air quality data. Its global coverage and daily observations make it useful for accessing trends of different pollutants in most parts of the world, which helps get information on different air pollutants while away from a specific place. The most important thing related to the Sentinel 5 satellite is that it helps provide air pollutant information transiently.

3.2 Processing

Hyperspectral remote sensing plays a crucial role in determining material properties by capturing spectral signatures across a wide range of wavelengths, enabling precise identification and analysis of surface and atmospheric components (Ahmed et al., 2024; Cavalli et al., 2011; Fan et al., 2020; Kokaly, 2012). The methodology for estimating NO_2 air pollutant concentrations using Sentinel-5P data involves several key steps. The measurement technique utilized is known as Differential Optical Absorption Spectroscopy (DOAS),

which works on the principle of selective absorption of light by atmospheric trace gases. It exploits the unique absorption features of gases like NO_2 and O_3 in the visible and ultraviolet spectrum. As sunlight passes through the atmosphere, these gases absorb light at specific wavelengths, allowing their concentrations to be identified and quantified by analyzing the differences between the measured and reference spectra (Anand et al., 2015; Chan et al., 2012; Platt et al., 2008).

First, Sentinel-5P satellite data is acquired in a slant direction along the satellite's look angle. The acquired data is then pre-processed to get improved accuracy and usability. This includes geolocation correction (adjustments made to ensure that each satellite observation is accurately mapped to its correct geographic location) and cloud and quality filtering (the removal of pixels affected by cloud cover, sensor noise, or other atmospheric interferences, to ensure that only reliable and clear-sky data are used for analysis) to ensure accuracy. The slant column densities (SCDs) of NO_2 are computed by fitting the absorption spectrum to the measured radiance captured by the satellite sensor along its line of sight through the atmosphere (Equation 1). This quantifies the total amount of NO_2 present along the slanted path from the Sun to the satellite sensor, encompassing both tropospheric and stratospheric components.

$$SCD = \int L.n(z)\,dz \qquad \text{…(Equation 1)}$$

L is the path length, and n(z) is the NO_2 number density as a function of altitude z. Further, the slant column density is converted to the vertical column density (VCD) using the air mass factor (Equation 2).

$$VCD = \frac{SCD}{AMF} \qquad \text{…(Equation 2)}$$

Where AMF is the air mass factor, AMF is a dimensionless quantity that depends on factors such as observation geometry, atmospheric conditions etc.. This process involves the hyperspectral measurement. AMF corrects for the viewing geometry and atmospheric scattering (Dimitropoulou, 2021). The obtained data is spatially averaged over specific grids to produce detailed maps with reliable information and reduced noise. Finally, yearly statistical metrics—minimum, maximum, mean, and standard deviation—were calculated to assess temporal changes and spatial variability. A distribution map of NO_2 concentrations was overlaid on the topographic map to identify high-concentration zones and pollution hotspots.

To evaluate NO_2 spatial distribution changes in Mumbai City, Sindhudurg, and Ratnagiri, NO_2 concentration maps for 2019–2023 were reclassified using the quantile method, creating equal-area classes ranging from very low to very high. The Global Moran's I formula was applied to determine the spatial association between yearly maps (Lee and Li, 2017; Zhang et al., 2008). Pairwise Global Correspondence values were computed to assess the similarity between distribution patterns for consecutive years. Statistical shifts were analyzed in relation to economic, industrial and lockdown periods. Distribution maps were then overlaid on a topographic map to identify spatial patterns in NO_2 concentration across the area.

For hazard zonation, a binary classification approach was applied to raster maps for each year from 2019 to 2023. A threshold concentration of 0.9×10^{-4} mol/m² was used to classify each pixel, where values below the threshold were assigned 0 (non-hazardous)

and values at or above the threshold were assigned 1 (hazardous). Subsequently, the classified raster maps for all years were combined using the raster calculator. The resulting composite map had pixel values ranging from 0 to 5, where 0 indicates no hazard over the five-year period, and 5 represents the most critical zones, consistently hazardous across all years.

4. Results and Discussions

4.1. General statistical analysis

Table 1. Spatial statistics of measured NO_2 of the Konkan region for different years. Values are in $*10^{-4}$ mole/sq.m.

Year	Minimum	Maximum	Mean	Standard deviation
2019	0.5388	1.6406	0.7027	0.1643
2020	0.5002	1.4266	0.6516	0.1377
2021	0.5619	1.6372	0.7217	0.1535
2022	0.5449	1.6577	0.7124	0.1633
2023	0.5964	1.7363	0.7680	0.1636

Table 1 summarizes the spatial statistics of NO_2 concentrations in the Konkan region from 2019 to 2023 (Figure 2). Figure 3 represents the NO_2 column density distribution over the region. It reveals trends in air pollution over time. The mean NO_2 concentration increased over the years, from 0.7027×10^{-4} mole/m² in 2019 to 0.7680×10^{-4} mole/m² in 2023, while the maximum concentration rose from 1.6406×10^{-4} mole/m² to 1.7363×10^{-4} mole/m². These changes indicate a regional trend of worsening air quality. It is particularly in hotspots with the highest pollution levels, such as Mumbai, Thane and its suburban area. Despite the rising concentrations, the standard deviation shows consistency over time. It suggests that the spatial distribution of NO_2 emissions did not change drastically over the area. However, the standard deviation in 2022 has decreased drastically with decrement of other parameters reflecting the impact of the COVID-19 lockdown.
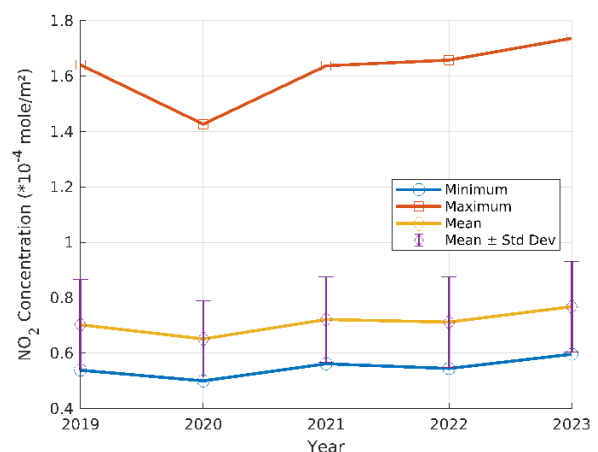

Figure 2. Various statistical parameters over the year.

The observed trends could be attributed to several factors. Increased urbanization and industrial activity in the Konkan region, including

growth in transportation networks and energy demands, likely contributed to higher NO_2 emissions. Seasonal meteorological conditions, such as reduced wind speeds or temperature inversions, may have exacerbated the concentration of pollutants in some years. Furthermore, any lapses in emission control measures or delays in adopting cleaner technologies could have intensified the issue. Conversely, the consistent standard deviation points to persistent emission sources, such as industrial zones or highways, maintaining similar spatial variability across the years.

Figure 3. Year-wise NO_2 column density distribution over the Konkan region.

4.2. Correspondence analysis

Table 2. Global measure of spatial association between the reclassified maps of NO_2 distribution over the Konkan region.

Year	2019	2020	2021	2022
2020	0.7974			
2021	0.7634	0.7549		
2022	0.7153	0.7150	0.7349	
2023	0.6470	0.6407	0.6485	0.7266

Table 2 presents the Global Correspondence values between reclassified maps of NO_2 distribution over the Konkan region from 2019 to 2023 calculated based on Global Moran's I (Figure 4). The quantile method ensured equal area under each class, as shown in Figure 5. The values indicate the degree of similarity in NO_2 spatial patterns between the corresponding years, with higher values reflecting stronger associations. For example, the spatial association between 2019 and 2020 is 0.7974, indicating highly similar NO_2 distribution patterns, while the association between 2019 and 2023 is lower at 0.6470, suggesting noticeable spatial changes over the years. Generally, closer consecutive years show higher associations (e.g., 0.7266 between 2022 and 2023), while associations decrease over longer time intervals, highlighting evolving spatial patterns in NO_2 distribution.
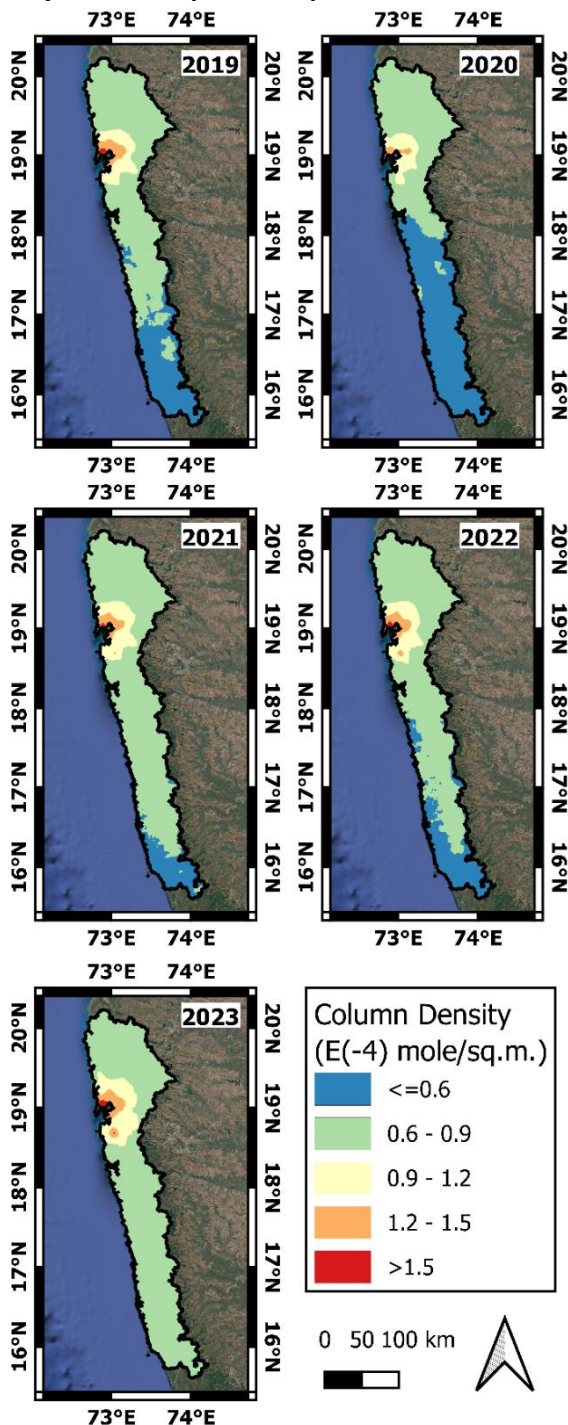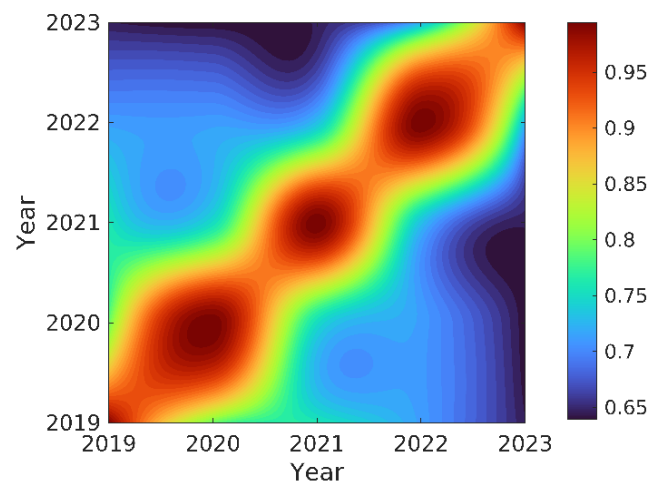

Figure 4. Continuous plot of global measure of spatial association showing declination over increasing time gap.

The observed trends can be attributed to several factors. The high association between consecutive years may result from consistent emission sources, such as industrial zones or urban areas, which tend to maintain similar spatial patterns over short periods. However, the decline in association over longer periods could stem from urban expansion, infrastructure development, or changes in emission regulations altering the spatial distribution of NO_2. Additionally, meteorological variations, such as wind patterns and seasonal rainfall, could influence pollutant dispersion, contributing to these observed changes. These factors indicate a dynamic

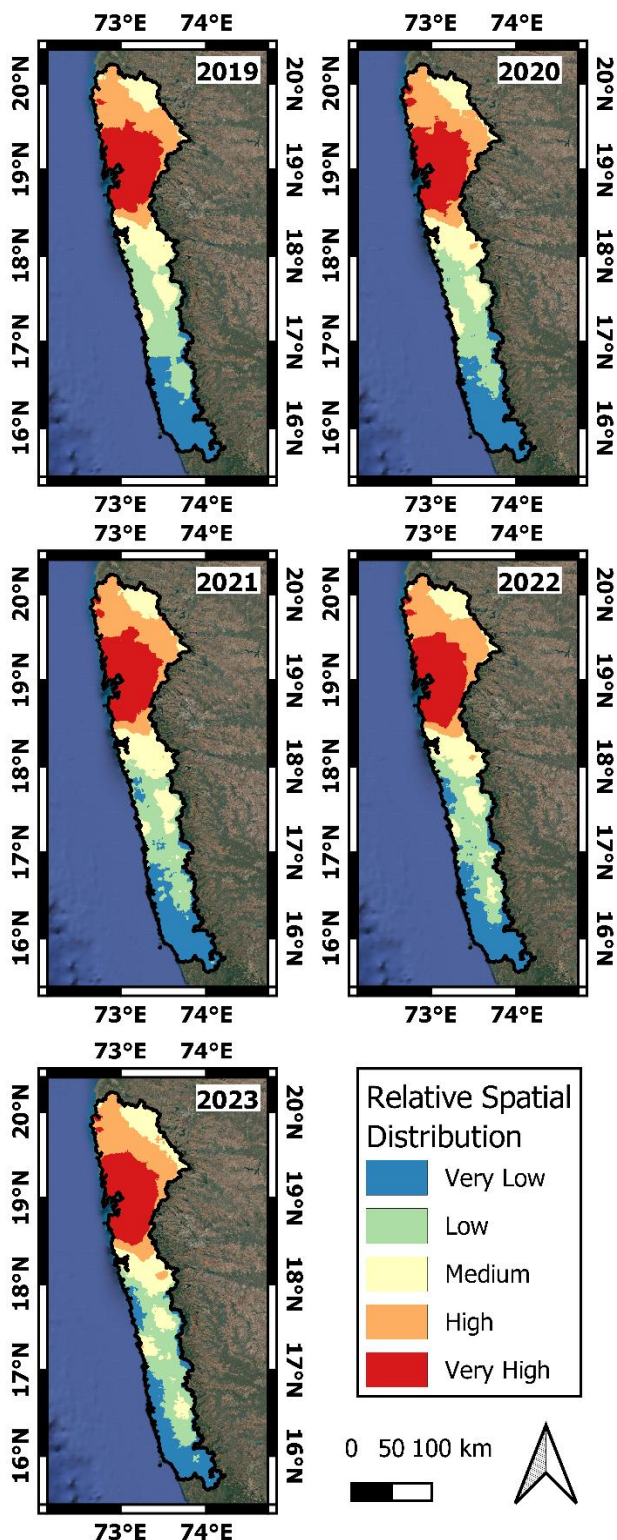interplay between anthropogenic activities and environmental conditions in shaping NO_2 distribution over time.

Figure 5. Relative spatial distribution of year-wise NO_2 over the Konkan region during the study period.

4.3. Hazard Zonation

Table 4. Area Distribution by Hazard Levels Based on NO_2 Concentration (2019–2023).

Hazard Level	Area (sq.km.)
0	26706
1	809
2	146
3	295
4	760
5	2065

The composite hazard zonation map provides a spatial representation of NO_2 concentration hotspots and their persistence over time (Table 4). Figure 6 shows the distribution of the study area in different hazard zones. The level of hazard indicates the year of consistency of the NO_2 over the area. The maximum persistency of NO_2 was observed in areas like Thane, Mumbai, Navi Mumbai, Washi, Dadar and Kolaba, which have level 5 hazards. It may be attributed to continuous vehicular emissions, industrial activity, port operations, and meteorological effects. These factors create a sustained high pollution level, classifying these regions as level 5 hazard zones in the composite hazard zonation map. Effective pollution control measures, such as strict emission norms, green infrastructure, and improved urban planning, are necessary to mitigate long-term exposure to NO_2.
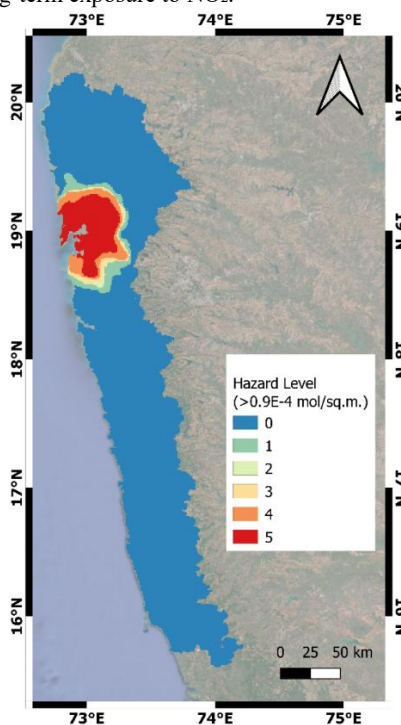

Figure 6. Hazard Zonation Map based on the consistency of NO_2 concentration during the study period.

5. Conclusion

The analysis of NO_2 concentrations over the Konkan region from 2019 to 2023 reveals a consistent and measurable increase in air pollution, with both mean and maximum concentration values rising over the years. Specifically, the mean NO_2 concentration increased from 0.7027×10^{-4} mole/m² in 2019 to 0.7680×10^{-4}

mole/m² in 2023, while the maximum value rose from 1.6406×10^{-4} to 1.7363×10^{-4} mole/m². Despite these increases, the standard deviation remained relatively stable, indicating that the spatial distribution of NO_2 emissions across the region did not fluctuate drastically, suggesting persistent emission sources such as industrial zones and transportation corridors. Spatial analysis using Global Moran's I further underscores the evolving distribution of NO_2. The degree of spatial association between consecutive years—such as 0.7974 (2019–2020) and 0.7266 (2022–2023)—is higher, whereas longer gaps show a decline, as seen in the reduced association between 2019 and 2023 (0.6470). This trend reflects gradual spatial shifts, likely driven by ongoing urban expansion, infrastructure development, and modifications in emission regulations or land-use practices. Seasonal meteorological influences, such as wind dispersion and rainfall, may also contribute to these evolving patterns.

The composite hazard zonation map highlights the persistence of NO_2 pollution hotspots, particularly in high-risk urban and industrial clusters such as Mumbai, Navi Mumbai, Thane, Washi, Dadar, and Kolaba. Areas falling under level 5 hazard zones—covering approximately 2065 sq. km—represent locations with sustained high concentrations throughout the study period. Additional zones, including levels 3 and 4, cover another 1055 sq. km combined, further demonstrating the spatial extent of air quality concerns. These findings emphasize the urgent need for region-specific and multi-layered mitigation strategies. Implementing stricter emission standards, investing in sustainable urban development, transitioning to cleaner fuels and transportation technologies, and improving environmental monitoring systems are critical to managing the growing air quality challenges in the Konkan region. Long-term planning should also integrate climate-sensitive urban policies to mitigate the effects of meteorological variability on pollutant dispersion.

Acknowledgement

References

Ahmed, I., Sharma, U.K., Garg, P.K., Thakur, A.K., 2024. Analysis of Cement properties using Hyperspectral Remote Sensing methods. ISPRS Ann. Photogramm. Remote Sens. Spat. Inf. Sci. 10, 15–20. https://doi.org/https://doi.org/10.5194/isprs-annals-X-4-2024-15-2024

Anand, J.S., Monks, P.S., Leigh, R.J., 2015. An improved retrieval of tropospheric NO2 from space over polluted regions using an Earth radiance reference. Atmos. Meas. Tech. 8, 1519–1535. https://doi.org/10.5194/amt-8-1519-2015

Behera, M.D., Mudi, S., Shome, P., Das, P.K., Kumar, S., Joshi, A., Rathore, A., Deep, A., Kumar, A., Sanwariya, C., 2022. COVID-19 slowdown induced improvement in air quality in India: rapid assessment using Sentinel-5P TROPOMI data. Geocarto Int. 37, 8127–8147.

Bhattacharjee, S., Garg, R.D., 2024. Estimation of sea ice drift and concentration during melt season using C-band dual-polarimetric Sentinel-1 data. Remote Sens. Appl. Soc. Environ. 33, 101104.

Bodah, B.W., Neckel, A., Maculan, L.S., Milanes, C.B., Korcelski, C., Ramírez, O., Mendez-Espinosa, J.F., Bodah, E.T., Oliveira, M.L.S., 2022. Sentinel-5P TROPOMI satellite application for NO2 and CO studies aiming at environmental valuation. J. Clean. Prod. 357, 131960.

Borkar, V.S., Gokhale, N.B., Dhopavkar, R. V, Khobragade, N.H., More, S.S., Kasture, M.C., 2018. Distribution of nutrients in different soil types in Konkan region of Maharashtra. Int. J. Chem. Stud 6, 275–279.

Bose, R.K., Leitmann, J., 1996. Environmental profile of the Singrauli region, India. Cities 13, 71–77. https://doi.org/10.1016/0264-2751(95)00127-1

Cavalli, R.M., Bassani, C., Palombo, A., Pascucci, S., Pignatti, S., Santini, F., 2011. Exploitation of hyperspectral data for infrastructures status assessment: Preliminary results of the istimes test bed, in: 2011 3rd Workshop on Hyperspectral Image and Signal Processing: Evolution in Remote Sensing (WHISPERS). IEEE, pp. 1–4.

Chan, C.K., Yao, X., 2008. Air pollution in mega cities in China. Atmos. Environ. 42, 1–42.

Chan, K.L., Pöhler, D., Kuhlmann, G., Hartl, A., Platt, U., Wenig, M.O., 2012. NO 2 measurements in Hong Kong using LED based long path differential optical absorption spectroscopy. Atmos. Meas. Tech. 5, 901–912.

Chore, H.S., Rupali, S., Kumar, G., 2021. Maharashtra, in: Geotechnical Characteristics of Soils and Rocks of India. CRC Press, pp. 429–450.

Chowdhury, A., Dwarakish, G.S., 2022. Selection of algorithm for land use land cover classification and change detection. IJARSCT 2, 15–24.

Dimitropoulou, E., 2021. Retrieval of the horizontal distributions of NO2, HCHO, and aerosols from urban MAX-DOAS measurements in support to air quality satellite validation.

Doke, A.B., 2017. Land Use/Cover Mapping of Konkan Region, Maharashtra. Int J Cur Res Rev| Vol 9, 1.

Fan, L., Fan, M., Alhaj, A., Chen, G., Ma, H., 2020. Hyperspectral imaging features for mortar classification and compressive strength assessment. Constr. Build. Mater. 251, 118935.

Gond, A.K., Jamal, A., Verma, T., 2024. Spatio-temporal trend analysis of air pollutants during COVID-19 over Korba district, Chhattisgarh (India) using Google Earth Engine. Remote Sens. Appl. Soc. Environ. 33, 101143. https://doi.org/10.1016/j.rsase.2024.101143

Gupta, K., Saha, A., Sen Gupta, B., 2024. Spatio-temporal distribution of pollutant trace gases (CO, CH4, O3 and NO2) in India: an observational study. Geol. Ecol. Landscapes 8, 306–326. https://doi.org/10.1080/24749508.2022.2132706

Guptha, G.C., Swain, S., Al-Ansari, N., Taloor, A.K., Dayal, D., 2022. Assessing the role of SuDS in resilience enhancement of urban drainage system: A case study of Gurugram City, India. Urban Clim. 41, 101075. https://doi.org/10.1016/j.uclim.2021.101075

Haque, M.S., Singh, R.B., 2017. Air pollution and human health in Kolkata, India: A case study. Climate 5, 77.

Hasan, M.M., Ahmed, A., 2023. Evaluation and Mapping the Atmospheric Air Quality of Coastal Area in Bangladesh Using Remote Sensing and GIS Techniques. Dhaka Univ. J. Earth Environ. Sci. 11, 53–64. https://doi.org/10.3329/dujees.v11i2.68840

Karanam, V., Motagh, M., Garg, S., Jain, K., 2021. Multi-sensor remote sensing analysis of coal fire induced land subsidence in Jharia Coalfields, Jharkhand, India. Int. J. Appl. Earth Obs. Geoinf. 102, 102439. https://doi.org/10.1016/j.jag.2021.102439

Kokaly, R.F., 2012. Spectroscopic remote sensing for material identification, vegetation characterization, and mapping, in: Algorithms and Technologies for Multispectral, Hyperspectral, and Ultraspectral Imagery XVIII. SPIE, pp. 311–322.

Kumar, K., Papnai, A., Kuri, M., Bhardwaj, A., 2022. Monitoring of Landslides between Tehri and Koteshwar Dams in Uttarakhand , Himalayas, in: International Dam Safety Conference, 10-12 October 2022, Jaipur, Rajasthan. pp. 10–12.

Lee, J., Li, S., 2017. Extending Moran's index for measuring spatiotemporal clustering of geographic events. Geogr. Anal. 49, 36–57.

Maltare, N.N., Vahora, S., 2023. Air Quality Index prediction using machine learning for Ahmedabad city. Digit. Chem. Eng. 7, 100093.

Mathew, A., Shekar, P.R., Nair, A.T., Mallick, J., Rathod, C., Bindajam, A.A., Alharbi, M.M., Abdo, H.G., 2024. Unveiling urban air quality dynamics during COVID-19: a Sentinel-5P TROPOMI hotspot analysis. Sci. Rep. 14, 21624.

Maurya, V.K., Dwivedi, R., Martha, T.R., 2022. Site scale landslide deformation and strain analysis using MT-InSAR and GNSS approach–A case study. Adv. Sp. Res. 70, 3932–3947.

Meo, S.A., Alqahtani, S.A., AlRasheed, R.A., Aljedaie, G.M., Albarrak, R.M., 2022. Effect of environmental pollutants PM2. 5, CO, O3 and NO2, on the incidence and mortality of SARS-COV-2 in largest metropolitan cities, Delhi, Mumbai and Kolkata, India. J. King Saud Univ. 34, 101687.

Mishra, A., Lal, B., Kumar, R., 2024. Air quality monitoring and its impact on local tree species in and around mining areas of Dhanbad District, Jharkhand, India, in: Spatial Modeling of Environmental Pollution and Ecological Risk. Elsevier, pp. 9–40.

Mondal, A., Paul, P.K., 2023. Monitoring of groundwater generated land subsidence by persistent scatterer analysis–A case study of the Kolkata Municipal Corporation (KMC), West Bengal. J. Earth Syst. Sci. 132, 181.

Nayak, G.N., Hanamgond, P.T., 2010. India, in: Encyclopedia of the World's Coastal Landforms. Springer, pp. 1065–1070.

Organization, W.H., 2021. WHO global air quality guidelines: particulate matter (PM2. 5 and PM10), ozone, nitrogen dioxide, sulfur dioxide and carbon monoxide. World Health Organization.

Pandey, A., Brauer, M., Cropper, M.L., Balakrishnan, K., Mathur, P., Dey, S., Turkgulu, B., Kumar, G.A., Khare, M., Beig, G., 2021. Health and economic impact of air pollution in the states of India: the Global Burden of Disease Study 2019. Lancet Planet. Heal. 5, e25–e38.

Platt, U., Stutz, J., Platt, U., Stutz, J., 2008. Differential absorption spectroscopy. Springer.

Pritipadmaja, Garg, R.D., Sharma, A.K., 2023. Assessing the cooling effect of blue-green spaces: implications for Urban Heat Island mitigation. Water 15, 2983.

Reshi, A.R., Moniruzzaman, M., Tripathi, A., Tiwari, R.K., Rahaman, K.R., 2022. A remote sensing based study of tropospheric ozone concentration amid COVID-19 lockdown over India using Sentinel-5P satellite data. Geocarto Int. 37, 17145–17164.

Sahu, A.K., Pradhan, P.K., Mohanty, C.R., Pradhan, M., 2020. Analysis of noise and air pollution in Sambalpur City, India, during Diwali. J. Environ. Eng. Sci. 15, 172–179. https://doi.org/10.1680/jenes.20.00006

Shabbir, Y., Guanhua, Z., Shah, S.R.A., Ishaq, R.A., 2024. Trans-boundary spatio-temporal analysis of Sentinel 5P tropospheric nitrogen dioxide and total carbon monoxide columns over Punjab and Haryana Regions with COVID-19 lockdown impact. Environ. Monit. Assess. 196, 291.

Sharifi, A., Felegari, S., 2022. Nitrogen dioxide (NO2) pollution monitoring with sentinel-5P satellite imagery over during the coronavirus pandemic (case study: Tehran). Remote Sens. Lett. 13, 1029–1039.

Sharma, R., Kumar, R., Sharma, D.K., Son, L.H., Priyadarshini, I., Pham, B.T., Tien Bui, D., Rai, S., 2019. Inferring air pollution from air quality index by different geographical areas: case study in India. Air Qual. Atmos. Heal. 12, 1347–1357.

Soudagar, R., Chowdhury, A., Bhardwaj, A., 2025. Enhanced large-

scale flood mapping using data-efficient unsupervised framework based on morphological active contour model and single synthetic aperture radar image. J. Environ. Manage. 380, 124836.

Srivastava, A., Thakur, A.K., Garg, R.D., 2025. An assessment of the spatiotemporal dynamics and seasonal trends in NO$_2$ concentrations across India using advanced statistical analysis. Remote Sens. Appl. Soc. Environ. 37, 101490. https://doi.org/10.1016/j.rsase.2025.101490

Suthar, G., Singhal, R.P., Khandelwal, S., Kaul, N., Parmar, V., Singh, A.P., 2022. Four-year spatiotemporal distribution & analysis of PM2. 5 and its precursor air pollutant SO2, NO2 & NH3 and their impact on LST in Bengaluru city, India, in: IOP Conference Series: Earth and Environmental Science. IOP Publishing, p. 12036.

Tang, T., Zhang, L., Zhu, H., Ye, X., Fan, D., Li, X., Tong, H., Li, S., 2024. Quantifying Urban Daily Nitrogen Oxide Emissions from Satellite Observations. Atmosphere (Basel). 15, 1–12. https://doi.org/10.3390/atmos15040508

Thakur, A.K., Attri, L., Garg, R.D., Jain, K., Kumar, D., Chowdhury, A., 2024. Temporal and Spatial Dynamics of Subsidence in Eastern Jharia, India, in: ISPRS Annals of the Photogrammetry, Remote Sensing and Spatial Information Sciences. Copernicus Publications Göttingen, Germany, pp. 349–356. https://doi.org/https://doi.org/10.5194/isprs-annals-X-4-2024-349-2024

Thakur, A.K., Garg, R.D., Jain, K., 2025a. An assessment of different line-of-sight and ground velocity distributions for a comprehensive understanding of ground deformation patterns in East Jharia coalfield. Remote Sens. Appl. Soc. Environ. 37, 101446. https://doi.org/10.1016/j.rsase.2024.101446

Thakur, A.K., Garg, R.D., Jain, K., 2025b. Land subsidence dynamics and its structural impact assessment over East Jharia, Jharkhand, India. J. Earth Syst. Sci. 134, 114. https://doi.org/10.1007/s12040-025-02564-8

Verma, D., Vijay, S., 2024. Time-Series Analysis of Dam Deformation Using Satellite-Based InSAR Technique: Case Studies from Oroville, Pong, and Tehri Dams, in: IGARSS 2024-2024 IEEE International Geoscience and Remote Sensing Symposium. IEEE, pp. 11136–11140.

Yaseen, Z.M., 2024. Flood hazards and susceptibility detection for Ganga river, Bihar state, India: Employment of remote sensing and statistical approaches. Results Eng. 21, 101665. https://doi.org/https://doi.org/10.1016/j.rineng.2023.101665

Zhang, C., Luo, L., Xu, W., Ledwith, V., 2008. Use of local Moran's I and GIS to identify pollution hotspots of Pb in urban soils of Galway, Ireland. Sci. Total Environ. 398, 212–221.

Zheng, Z., Yang, Z., Wu, Z., Marinello, F., 2019. Spatial variation of NO2 and its impact factors in China: An application of sentinel-5P products. Remote Sens. 11, 1939.

Савенець, М.В., Дворецька, І.В., Надточій, Л.М., 2019. Current state of atmospheric air pollution in Ukraine based on Sentinel-5P satellite data. Visnyk VN Karazin Kharkiv Natl. Univ. Ser. Geol. Geogr. Ecol. 221–233.